Robo2 Predicts a Better Prognosis and Inhibits Malignant Behavior in Vivo in Pancreatic Ductal Adenocarcinoma

Cheng Ding
Peking Union Medical College Hospital
Yatong Li
Peking Union Medical College Hospital
Shunda Wang
Peking Union Medical College Hospital
Cheng Xing
Peking Union Medical College Hospital
Lixin Chen
Peking Union Medical College Hospital
Hanyu Zhang
Peking Union Medical College Hospital
Yizhi Wang
Peking Union Medical College Hospital
MengHua Dai (daimh@pumch.cn)
Peking Union Medical College Hospital https://orcid.org/0000-0002-5911-5588

Primary research

Keywords: SLIT/ROBO, ROBO2, PDAC, RT-PCR

Posted Date: January 20th, 2021

DOI: https://doi.org/10.21203/rs.3.rs-148994/v1

Abstract

Background

Pancreatic ductal adenocarcinoma (PDAC) is a lethal malignancy with an extremely poor prognosis and a high mortality rate. Genome-wide studies have shown that the SLIT/ROBO signaling pathway plays an important role in pancreatic tumor development and progression. However, the effect and mechanism of ROBO2 in the progression of pancreatic cancer remains largely unknown.

Methods

In this study, real-time polymerase chain reaction (RT-PCR) and western blot analyses were adopted to evaluate the expression level of ROBO2 and proteins in pancreatic cell lines. Cell migration and invasion and cell proliferation were conducted in AsPC-1 and MIA PaCa-2 cell lines. RNA sequencing and western blot were undertaken to explore the mechanisms and potential targeted molecules. ROBO2 expression in tumor tissues was evaluated by immunohistochemistry in 95 patients.

Results

ROBO2 expression was downregulated in PDAC cell lines and tissue samples. A high level of ROBO2 was associated with good overall survival. Upregulation of ROBO2 inhibited PDAC cell proliferation, migration, and invasion, whereas the opposite results were found in the ROBO2 downregulation group. In addition, xenograft animal models further confirmed the effect of ROBO2 on proliferation. Finally, the RNA sequencing results indicated that ROBO2 facilitates anti-tumorigenicity partly via inhibiting ECM1 in PDAC.

Conclusions

Our work suggests that ROBO2 inhibits tumor progression in PDAC and may serve as a predictive biomarker and therapeutic target in PDAC.

Introduction

Pancreatic ductal adenocarcinoma (PDAC), commonly known as pancreatic cancer, is becoming the main cause of cancer-related death because of its poor prognosis [1, 2]. The difficulty of early diagnosis and the fact that nearly 80–85% of patients have no opportunity to undergo surgery at the time of diagnosis are major obstacles to long-term survival [3]. Carbohydrate antigen 19 − 9 is the most important tumor marker in PDAC [4]. Therefore, elucidation of the molecular mechanisms underlying the development and progression of PDAC and identification of additional promising biomarkers may improve the prognosis.

The roundabout (ROBO) family comprises single-pass transmembrane proteins belonging to the immunoglobulin superfamily. The extracellular domain of ROBO2 contains five immunoglobulin-like

domains followed by three fibronectin domains as well as an intracellular region that consists of four conserved cytoplasmic domains. ROBO2 plays important role in many tissues during development and particularly in the nervous system. Recent studies have demonstrated that ROBO2 is dysregulated in various cancers such as gastric cancer [5], acute myeloid leukemia [6], colorectal cancer [7], prostate cancer [8], ovarian cancer [9], and breast cancer [10]. However, the exact effect of ROBO2 in PDAC remains unclear.

In the present study, we explored the functions of ROBO2 alterations in tumor progression and the possible underlying mechanisms. As far as we know, this is the first study to explore the biological roles of ROBO2 in PDAC.

Materials And Methods

Clinical specimens and immunohistochemistry

In the aggregate, 95 tumor tissues were obtained from Peking Union Medical College Hospital (PUMCH) from November 2008 to September 2015. This study was authorized by the ethics committee of PUMCH and all patients provided written informed consent. The tissue microarray was constructed as described previously [11]. ROBO2 expression level was evaluated by immunohistochemistry using rabbit anti-human ROBO2 polyclonal antibodies at 1:300 dilution (ab75014; Abcam, Cambridge, UK). Two pathologists who were blinded to the clinicopathological data evaluated the sections independently. In the case of discrepancies, joint evaluation was performed to reach a consensus. The *H*-score, a combination of the percentage of positively stained cells and the staining intensity, was applied for further evaluation. The *H*-score ranged from 0 to 300, and the optimal cutoff value for the *H*-score reflecting a high/low ROBO2 expression level was defined by the largest Youden's index within the receiver operating characteristic curve. The clinicopathological data, including the patients' characteristics, tumor status, and complete prognosis date, are summarized in Table 1.

Cell culture

Human PDAC cell lines (PANC-1, MIA PaCa-2, CFPAC-1, SW1990, BxPC-3, and AsPC-1) and the immortalized normal pancreatic cell line HPNE were obtained from the American Type Culture Collection (Manassas, VA, USA) and maintained in Dulbecco's modified Eagle's medium, Iscove's Modified Dulbecco's Medium, and Roswell Park Memorial Institute 1640 medium (HyClone, Logan, UT, USA) supplemented with 10% fetal bovine serum (Gibco, Thermo Fisher Scientific, Waltham, MA, USA) at 37°C with 5% carbon dioxide in a cell culture incubator.

Transfection

MIA PaCa-2 and PANC-1 cells were transfected with siRNA targeting ROBO2 and a scramble control siRNA. Transient transfections were performed using Lipofectamine 3000 (Thermo Fisher Scientific) according to the manufacturer's protocol. MIA PaCa-2 and ASPC-1 cells were seeded in 6-well plates and

cultured until the confluence reached 60-70%. They were then transfected with an ROBO2-knockdown lentivirus (termed SH), scrambled control lentivirus (termed NSH), ROBO2 overexpression lentivirus (termed OE), or negative control lentivirus (termed NOE). Lentivirus constructions of ROBO2 knockdown and overexpression were purchased from GenePharma (Shanghai, China). Quantitative real-time polymerase chain reaction (qRT-PCR) and western blot assays were performed to evaluate the specificity and efficiency of the transfections.

RNA isolation and qRT-PCR

PDAC cells were seeded in 6-well plates at 5×10^5 cells/well and transfected for 36 hours. Total RNA was extracted with TRIzol reagent. PrimeScript™ RT Master Mix (Takara Bio, Shiga, Japan) and an SYBR Green PCR Kit (Thermo Fisher Scientific) were applied for reverse transcription and qRT-PCR assays in accordance with the manufacturers' instructions. The ROBO2 primers was as follows: forward, 5'-GAGACCTCACAATCACCAACATTCAAC-3'; reverse, 5'-CAGTAACGCTGTACCATCCACTGC-3'; β-actin forward, 5'-TGAAGGTAGTTTCGTGGATGC-3'; and β-actin reverse, TCCCTGGAGAAGAGCTACGA.

Western blot

Cultured cells were lysed in RIPA buffer supplemented with a proteinase inhibitor cocktail. A bicinchoninic acid kit was used to calculate the protein concentration. The lysate containing approximately 20.0 μg of protein was loaded onto 8% SDS-PAGE gel and then run for 2 hours at 90 V. Proteins were transferred to Immobilon-PVDF membranes (EMD Millipore, Burlington, MA, USA) at 400 mA for 1.5 hours. After blocking with 5% non-fat milk at room temperature, the membranes were incubated with the following primary antibodies: anti-ROBO2 antibody at 1:1000 dilution (ab75014; Abcam) and anti-GAPDH antibody at 1:2000 dilution (60004-1-Ig; Proteintech, Rosemont, IL, USA). In addition, the following antibodies were used: anti-NF-κB P65 antibody (66535-1-Ig; Proteintech), anti-ECM1 antibody (11521-1-AP; Preoteintech), anti-N-cadherin antibody (13116; Cell Signaling Technology, Danvers, MA, USA), anti-E-cadherin antibody (14472; Cell Signaling Technology), and anti-vimentin antibody (5471; Cell Signaling Technology).

Next, we washed the membranes four times for 10 minutes each in TBS-T at room temperature and then incubated with secondary antibodies for 1.5 hours in 5% non-fat milk at room temperature. Finally, the membranes were washed four times for 10 minutes each in TBS-T and visualized by exposure to an enhanced chemiluminescence system.

Cell Counting Kit-8 (CCK-8) assay

Cancer cells were planted in 96-well plates at 3×10^3 cells/well, and 10 μL/well of CCK-8 reagent (Dojindo, Kumamoto, Japan) was added 0, 24, 48, 72, and 96 hours later. After 2 hours of incubation at 37°C, we used a microplate reader to calculate the absorbance at an optical density (OD) of 450 to 630 nm.

Wound healing and Transwell migration and invasion assays

A wound healing assay was used to examine the ability of cell migration. After the cells reached 80% to 90% confluence in the six-well plates, they were wounded by scratching with a 200-μl disposable pipette tip and washed twice with phosphate-buffered saline (PBS). The wounds were photographed at 0, 24, and 48 hours with a DFC300 FX microscope (Leica, Wetzlar, Germany), and their widths were quantitated with ImageJ software (National Institutes of Health, Bethesda, MD, USA).

Transwell migration and invasion assays were performed in 24-well Transwell plates (Corning) inculuding a polycarbonate membrane (8-μm pore size). About 1×10^4 cells were plated in the top chamber after transfection. Medium containing 10% PBS was added to the lower chambers. After incubation at 37°C for 36 hours, the non-invading cells were gently removed with a cotton swab, and the penetrated cells were fixed in methanol for 20 minutes and stained with hematoxylin and eosin for 10 and 5 minutes, respectively. Cell numbers were counted under a DFC300 FX microscope (Leica).

Colonial formation

500 MIA PaCa-2 or AsPC-1 cells were plated in 6-well plates. And two weeks later, the cells were fixed in methanol for 20 minutes and stained with hexamethylpararosaniline for 10 minutes.

RNA sequencing

Total RNA was extracted from samples using TRIzol, and the RNA quality was determined by examining A260/A280 with a Nanodrop™ One^C spectrophotometer (Thermo Fisher Scientific). The kit eliminates duplication bias in PCR and sequencing steps by using a unique molecular identifier of eight random bases to label the pre-amplified cDNA molecules. All data were analyzed according to the manufacturers' instructions by Seqhealth Technology Co., Ltd. (Wuhan, China). Differentially expressed genes were then identified by a false discovery rate-corrected p-value cutoff of 0.05 and fold-change cutoff of 2. Gene ontology analysis and Kyoto Encyclopedia of Genes and Genomes (KEGG) enrichment analysis were performed.

Animal experiments

All animal experiments were approved by the PUMCH Animal Care and Use Committee. MiaPaCa-2 cells stably transfected with shROBO2 or shNC and AsPC-1 cells stably transfected with oeROBO2 or oeNC were subcutaneously injected into the left back of 5-week-old female BALB/c mice (5×10^6 cells in 150 μL of PBS). The tumor size was measured twice a week, and the volume was calculated using the following formula: volume (mm^3) = 1/2 × length × width^2 The animals were euthanized 4 to 5 weeks later.

Statistical analysis

Statistical analysis and graph representations were performed using SPSS v.22.0 software (IBM Corp., Armonk, NY, USA) and GraphPad Prism 7 Software (GraphPad, San Diego, CA, USA), respectively. Each experiment was repeated at least three times. Continuous variables are presented as mean ± standard

deviation. Categorical data were compared using the chi-square test. The level of statistical significance was set at a *P* value of <0.05.

Results

Downregulation of ROBO2 expression in PDAC

The pancreatic cell line HPNE and six PDAC cell lines were used to investigate ROBO2 expression by western blot and RT-PCR (Figures 1A, B). HPNE cells had the highest ROBO2 expression, followed by PANC-1 and MIA PaCa-2 cells. AsPC-1 and BxPC-3 had lower ROBO2 expression. Based on these results, PANC-1, MIA PaCa-2, and AsPC-1 cells were selected for further analysis. ROBO2 knockdown (ROBO2-SH) and overexpression (ROBO2-OE) cell lines were established by transfection of MIA PaCa-2 and AsPC-1 cells. Transfection efficacy in the ROBO2-SH and ROBO2-OE cells lines was compared with that in the control cell lines and confirmed by western blot and RT-PCR (Figures 1C, D).

Restraint of pancreatic cell proliferation *in vitro*

CCK-8 assays were applied to investigate the roles of ROBO2 on proliferation. The proliferation assay showed that ROBO2 downregulation promoted the cell proliferation capacity compared with NSH in MIA PaCa-2 stable cell lines, whereas ROBO2 overexpression significantly inhibited proliferation in AsPC-1 cells (Figure 2A). The clonal formation assays showed similar results (Figure 2B).

Inhibition of pancreatic cancer cell migration and invasion *in vitro*

The migration and invasion abilities of ROBO2-SH and ROBO2-OE cell lines were evaluated by wound healing and Transwell migration and invasion assays *in vitro.* Wound healing assays revealed that ROBO2 knockdown significantly shortened the wound healing time in MIA PaCa-2 cell lines; however, ROBO2 overexpression increased migratory activity in AsPC-1 cell lines compared with control cells (Figure 3A). Transwell migration and invasion assays were performed to further validate these results. ROBO2 knockdown significantly promoted the migration and invasion of MIA PaCa-2 cells, and ROBO2 overexpression decreased the migration and invasion ability of AsPC-1 cells (Figures 3B, C). We also further investigated the role of ROBO2 in epithelial–mesenchymal transition (EMT). ROBO2 downregulation increased the expression of vimentin and N-cadherin, and ROBO2 upregulation increased the expression of E-cadherin (Figure 3D).

Expression level of ROBO2 in tumor tissues and its association with a better prognosis in patients with PDAC

We investigated the level of ROBO2 expression in 95 samples by immunohistochemistry (Figures 4A, B). First, we evaluated the association between the expression of ROBO2 and clinicopathologic features. The clinicopathological parameters are summarized in Table 1. ROBO2 expression was not significantly correlated with age, sex, tumor size, location, or T or N stage.

Next, we evaluated the association between ROBO2 expression and the prognosis. Kaplan–Meier analysis showed that patients with high ROBO2 expression had significantly better disease-free survival and overall survival than those with low ROBO2 expression (Figures 4C, D). Univariate analysis and multivariable analysis revealed that the ROBO2 expression level was positively associated with disease-free survival and overall survival. Overall, our data indicated that the ROBO2 expression level might be an independent predictor of overall survival.

Inhibition of PDAC cell proliferation *invivo*

We used a xenograft tumor model to investigate the effect of ROBO2 on cell proliferation *in vivo.* Stably transfected MIA PaCa-2 and AsPC-1 cells were injected into nude mice. After observation for 4 weeks (MIA PaCa-2 group) and 5 weeks (AsPC-1 group), the results showed that ROBO2 knockdown promoted tumor growth while ROBO2 overexpression inhibited tumor growth (Figures 5A, B, C). ROBO2 mRNA and protein expression were detected by RT-qPCR and immunohistochemistry (Figures 5D, E). In summary, these PDAC cell line xenografts indicated that ROBO2 is remarkably correlated with the proliferation ability of PDAC cells *in vivo.*

RNA sequence and mechanism

To further investigate the potential mechanisms underlying how ROBO2 affects the biological behavior of pancreatic cancer, mRNA expression profiling was performed in ROBO2-overexpression cell lines (Figure 6A). Gene ontology analysis and KEGG analysis of differentially expressed genes were performed. Genes regulated by ROBO2 were involved in biological process, cellular component, and molecular functions (Figures 6B, C, D). Western blot was performed to further investigate the effect of ROBO2 on the extracellular matrix (ECM), revealing that the level of ECM protein 1 (ECM1) in the ROBO2-OE was significantly lower than that in the ROBO2-NC, and vice versa in the ROBO2-SH (Figure 6E). Overall, our superficial results suggest that ROBO2 might inhibit PDAC progression by inhibiting ECM1; however, further experiments are needed to confirm these findings.

Discussion

Because of delayed diagnosis and early metastasis, pancreatic cancer remains an extremely malignant carcinoma. Novel targets and biomarkers are required for the treatment of pancreatic cancer. In the present study, we explored the expression and effect of ROBO2 in pancreatic cancer. We first evaluated the mRNA and protein expression levels of ROBO2 in the normal pancreatic cell line HPNE and six pancreatic cancer cell lines and found that ROBO2 expression was lower in the pancreatic cancer cell lines. Clinicopathologic analysis showed that increased ROBO2 expression was correlated with a better prognosis. Downregulation of ROBO2 promoted proliferation and migration *in vitro* and accelerated tumor growth *in vivo*. mRNA sequencing showed that ROBO2 downregulated the expression of ECM1, promoting the migration and invasion of pancreatic cancer.

The SLIT/ROBO signaling pathway, which was initially identified through its effect on axon guidance [12], has shown dual roles in cancers by affecting both oncogenes and anti-tumor genes. In colorectal cancer, the levels of ROBO1 and ROBO4 are significantly higher in tumor tissues than para-tumor tissues. ROBO1 is expressed mainly in tumor cells, while ROBO4 is situated in endothelial cells of tumor vessels [13]. In breast cancer, the SLIT2/ROBO1 signaling pathway enhances the invasion and migration of cancer cells by promoting matrix metalloproteinase 9 [14]. Additionally, the SLIT/ROBO pathway has been shown to act on tumor suppressor genes in some special cancers. The SLIT2 gene is downregulated in colorectal cancer, and high SLIT2 expression can inhibit the migration capability [15]. Accordingly, overexpression of SLIT2 can inhibit migration and invasion of melanoma cells and immortalized epithelial cells by reducing Cdc-42 activation and preventing hepatocyte growth factor-induced dynamic responses [16]. In lung cancer cells, low expression of USP33 was associated with a poor prognosis, which may be attributed to the instability of the ROBO1 protein [17]. Thus, clarification of this contradictory effect may be of great significance for the treatment of pancreatic cancer.

As a member of the immunoglobulin superfamily, ROBO2 consists of three parts: the extracellular domain, transmembrane regions, and the intracellular region. ROBO2 has been found to regulate different physiological functions and tumor development. Gonçalves et al. [18] revealed an important role of ROBO2 in lung development. Escot et al. [19] found that ROBO2 plays an important role in pancreas cell identity and plasticity. In the developing mouse embryo, simultaneous knockout of ROBO1 and ROBO2 resulted in a decreased pancreatic volume.

The functions and mechanisms of ROBO2 in tumor progression are gradually being recognized. Skuja et al. found that ROBO2 deletion was identified in more than half of patients with metastatic colorectal cancer [20]. However, through L1-targeted resequencing of colorectal tumors and matched normal DNA, Solyom et al. described ROBO2 as an oncogene [21]. Generally, ROBO2 suppresses WNT/β-catenin signaling activity and inhibits migration and invasion of cancer cells [22,23]. Biankin et al. revealed that high expression of ROBO2 was associated with a better prognosis, which is consistent with our results. Furthermore, transforming growth factor (TGF)-β activation promoted the progression of pancreatic cancer [24]. Pinho et al. reported that in acute pancreatitis mouse models, the absence of ROBO2 from epithelial cells may result in the activation of TGF-β and promote a strong anti-inflammatory response and that these effects can be reversed by the TGF-β inhibitor galunisertib [25]. Han et al. found that ROBO3 expression was upregulated in PDAC tissue samples and that the level of ROBO3 was positively correlated with the tumor stage. Moreover, the overexpression of ROBO3 promoted malignant biological behavior of pancreatic cancer both *in vitro* and *in vivo* and activated the WNT/β-catenin signaling pathway. However, their study did not show a significant relationship between the ROBO3 expression level and overall survival or disease-free survival [26].

ECM1 overexpression is related to strong malignant behavior and a poor prognosis in multiple malignancies, such as gastric cancer, breast cancer, laryngeal carcinoma, hepatocellular carcinoma, and others [27-30]. Various regulatory mechanisms are involved in the migration of malignant tumors, and EMT is one such mechanism of great importance [31]. The main features of EMT are loss of the epithelial

phenotype and acquisition of the mesenchymal phenotype, resulting in enhanced tumor cell migration and invasiveness via impaired cell–matrix adhesion and remodeling of the ECM [32-35]. E-cadherin, N-cadherin, and vimentin, important markers of EMT, are associated with the metastatic phenotype. Our study also showed that ROBO2 expression was negatively associated with EMT. Lee et al. reported that ECM1 could advance EMT progression via stabilization of the β-catenin protein in metastatic breast cancer. Their study also demonstrated that ECM1 regulates chemotherapy resistance, sphere-forming ability, and cancer stem cell maintenance [36]. Wu et al. reported that ECM1 could interact with moesin to promote aggressive breast cancer phenotypes [37]. Another primary study showed that migration and metastasis of cancer cells may be induced by a simple change in the structure of the ECM [38]. These findings are consistent with the results of our study, suggesting that ROBO2 has anti-cancer effects in pancreatic cancer.

We acknowledge that our study has some limitations. First, the pancreatic cancer tissues were obtained from surgical resection, and because of the low resection rate, bias in the association between ROBO2 expression and the TNM stage is inevitable. Additionally, the sample size was not large (<100 patients). Second, although RNA sequencing and bioinformatics were used to analyze the potential targeted genes of ROBO2, the mechanism by which ROBO2 downregulates the expression of ECM1 is still unknown. Deeper and more direct proofs are needed to demonstrate the signaling pathway regulated by ROBO2 and the mechanism of ROBO2 in the development of pancreatic cancer. Third, although RNA sequencing and analysis is used to investigate many genes involved in cellular metabolism, we did not investigate the functions and effects of ROBO2 in pancreatic cancer metabolism. Further studies are needed to investigate the role and mechanism of ROBO2 in pancreatic tumor metabolism.

In summary, our results suggest that ROBO2 inhibits malignant biological behaviors, including cell proliferation and migration. We found relevance between the overexpression of ROBO2 and benign cancer behaviors and a better prognosis in patients with pancreatic cancer. Our study indicates that ROBO2 acts as a tumor suppressor gene and can potentially be a therapeutic target for pancreatic cancer. Protein chip and tissue microarray of ROBO2 may be used to predict the survival of patients with PDAC.

Declarations

Ethics approval and consent to participate

Written informed consent was obtained from individual or guardian participants. The study was approved by the Ethics Committee of Peking Union Medical College Hospital.

Consent for publication

Not applicable.

Availability of data and materials

All data generated or analyzed during this study are included in this published article.

Competing interests

The authors declare that they have no competing interests

Funding

This work was supported by the project of National Natural Science Foundation of China (81903150 & 82073238)

the project of CAMS Innovation Fund for Medical Sciences (2016-I2M-3-005)

the project of National Major Research and Development Programs of the Ministry of Science and Technology of China (2017YFC1308602)

Authors' contributions

MD designed concept of this manuscript. CD conducted the experiments and drafted the manuscript. YL reviewed the manuscript and made revisions on the drafts. CX and CD contributed to verify the data analysis. LC scrutinized the data. YW and HZ prepared the pathological analysis. All authors approved the final version.

Acknowledgments

The authors thank all of the staff from the Department of General Surgery and Department of Pathology, Peking Union Medical College Hospital.

References

[1] Chen W, Zheng R, Baade P D, et al. Cancer statistics in China, 2015[J]. CA: A Cancer Journal for Clinicians, 2016, 66(2).

[2] Siegel R L, Miller K D, Jemal A. Cancer statistics, 2020[J]. CA: A Cancer Journal for Clinicians, 2020, 70(1).

[3] Li D, Xie K, Wolff R, Abbruzzese JL. Pancreatic cancer. Lancet. (2004) 363:1049–57

[4] Gu X, Zhou R, Li C, et al. Preoperative maximum standardized uptake value and carbohydrate antigen 19–9 were independent predictors of pathological stages and overall survival in Chinese patients with pancreatic duct adenocarcinoma[J]. BMC Cancer, 2019, 19.

[5] Chang Z W, Dong L, Qin Y R, et al. Correlations between gastric cancer family history and ROBO2 and RASSF2A gene methylations. [J]. Journal of Cancer Research and Therapeutics, 2016, 12(2):597.

[6] Aleksandra, Gołos, Dorota, et al. The Expression of the SLIT-ROBO Family in Adult Patients with Acute Myeloid Leukemia. [J]. Archivum immunologiae et therapiae experimentalis, 2019.

[7] Je E M, Gwak M, Oh H, et al. Frameshift mutations of axon guidance genes ROBO1 and ROBO2 in gastric and colorectal cancers with microsatellite instability. [J]. Pathology, 2013, 45(7):645.

[8] Choi Y J, Yoo N J, Lee S H. Down-regulation of ROBO2 Expression in Prostate Cancers[J]. Pathology & Oncology Research, 2013.

[9] Dickinson, Rachel, E, et al. Glucocorticoid Regulation of SLIT/ROBO Tumour Suppressor Genes in the Ovarian Surface Epithelium and Ovarian Cancer Cells. [J]. Plos One, 2011.

[10] Anil, Prasad, Aaron, et al. Slit Protein-mediated Inhibition of CXCR4-induced Chemotactic and Chemoinvasive Signaling Pathways in Breast Cancer Cells[J]. Journal of Biological Chemistry, 2003.

[11] lu J, Zhou L, You L, et al. Clinicopathological and prognostic significance of MKK4 and MKK7 in resectable pancreatic ductal adenocarcinoma[J]. Human Pathology, 2019, 86:143-154.

[12] Nguyen-Ba-Charvet KT, Chédotal A. Role of Slit proteins in the vertebrate brain. J Physiol Paris. 2002 Jan-Mar;96(1-2):91-8.

[13] Gröne J, Doebler O, Loddenkemper C, Hotz B, Buhr HJ, Bhargava S. Robo1/Robo4: differential expression of angiogenic markers in colorectal cancer. Oncol Rep. 2006 Jun;15(6):1437-43.

[14] Schmid BC, Rezniczek GA, Fabjani G, Yoneda T, Leodolter S, Zeillinger R. The neuronal guidance cue Slit2 induces targeted migration and may play a role in brain metastasis of breast cancer cells. Breast Cancer Res Treat. 2007 Dec;106(3):333-42.

[15] Huang Z, Wen P, Kong R, Cheng H, Zhang B, Quan C, Bian Z, Chen M, Zhang Z, Chen X, Du X, Liu J, Zhu L, Fushimi K, Hua D, Wu JY. USP33 mediates Slit-Robo signaling in inhibiting colorectal cancer cell migration. Int J Cancer. 2015 Apr 15;136(8):1792-802.

[16] Stella MC, Trusolino L, Comoglio PM. The Slit/Robo system suppresses hepatocyte growth factor-dependent invasion and morphogenesis. Mol Biol Cell. 2009 Jan;20(2):642-57.

[17] Wen P, Kong R, Liu J, Zhu L, Chen X, Li X, Nie Y, Wu K, Wu JY. USP33, a new player in lung cancer, mediates Slit-Robo signaling. Protein Cell. 2014 Sep;5(9):704-13.

[18] Gonçalves AN, Correia-Pinto J, Nogueira-Silva C. ROBO2 signaling in lung development regulates SOX2/SOX9 balance, branching morphogenesis and is dysregulated in nitrofen-induced congenital diaphragmatic hernia. Respir Res. 2020 Nov 18;21(1):302.

[19] S. Escot, D. Willnow, H. Naumann et al.., “Robo signalling controls pancreatic progenitor identity by regulating tead transcription factors,” *Nature Communications*, vol. 9, no. 1, 2018.

[20] Skuja E, Butane D, Nakazawa-Miklasevica M, Daneberga Z, Purkalne G, Miklasevics E. Deletions in metastatic colorectal cancer with chromothripsis. Exp Oncol. 2019 Dec;41(4):323-327.

[21] Solyom S, Ewing AD, Rahrmann EP, Doucet T, Nelson HH, Burns MB, Harris RS, Sigmon DF, Casella A, Erlanger B, Wheelan S, Upton KR, Shukla R, Faulkner GJ, Largaespada DA, Kazazian HH Jr. Extensive somatic L1 retrotransposition in colorectal tumors. Genome Res. 2012 Dec;22(12):2328-38.

[22] Biankin AV, Waddell N, Kassahn KS et al. Pancreatic cancer genomes reveal aberrations in axon guidance pathway genes. Nature. 2012 Nov 15;491(7424):399-405.

[23] Waddell N, Pajic M, Patch AM, et al. Whole genomes redefine the mutational landscape of pancreatic cancer. Nature. 2015 Feb 26;518(7540):495-501.

[24] Achyut BR, Yang L. Transforming growth factor-β in the gastrointestinal and hepatic tumor microenvironment. Gastroenterology. 2011 Oct;141(4):1167-78.

[25] Pinho AV, Van Bulck M, Chantrill L, et al. ROBO2 is a stroma suppressor gene in the pancreas and acts via TGF-β signalling. Nat Commun. 2018 Nov 30;9(1):5083.

[26] Han S, Cao C, Tang T, Lu C, Xu J, Wang S, Xue L, Zhang X, Li M. ROBO3 promotes growth and metastasis of pancreatic carcinoma. Cancer Lett. 2015 Sep 28;366(1):61-70.

[27] Gan L, Meng J, Xu M, Liu M, Qi Y, Tan C, Wang Y, Zhang P, Weng W, Sheng W, Huang M, Wang Z. Extracellular matrix protein 1 promotes cell metastasis and glucose metabolism by inducing integrin β4/FAK/SOX2/HIF-1α signaling pathway in gastric cancer. Oncogene. 2018 Feb 8;37(6):744-755.

[28] Lal G, Hashimi S, Smith BJ, Lynch CF, Zhang L, Robinson RA, Weigel RJ. Extracellular matrix 1 (ECM1) expression is a novel prognostic marker for poor long-term survival in breast cancer: a Hospital-based Cohort Study in Iowa. Ann Surg Oncol. 2009 Aug;16(8):2280-7.

[29] Gu M, Guan J, Zhao L, Ni K, Li X, Han Z. Correlation of ECM1 expression level with the pathogenesis and metastasis of laryngeal carcinoma. Int J Clin Exp Pathol. 2013 May 15;6(6):1132-7.

[30] Chen H, Jia WD, Li JS, Wang W, Xu GL, Ma JL, Ren WH, Ge YS, Yu JH, Liu WB, Zhang CH, Wang YC. Extracellular matrix protein 1, a novel prognostic factor, is associated with metastatic potential of hepatocellular carcinoma. Med Oncol. 2011 Dec;28 Suppl 1: S318-25.

[31] Guarino M. Epithelial-mesenchymal transition and tumour invasion. Int J Biochem Cell Biol. 2007;39(12):2153-60.

[32] Thompson EW, Newgreen DF, Tarin D. Carcinoma invasion and metastasis: a role for epithelial-mesenchymal transition? Cancer Res. 2005 Jul 15;65(14):5991-5;

[33] Chen HT, Liu H, Mao MJ, Tan Y, Mo XQ, Meng XJ, Cao MT, Zhong CY, Liu Y, Shan H, Jiang GM. Crosstalk between autophagy and epithelial-mesenchymal transition and its application in cancer therapy. Mol Cancer. 2019 May 24;18(1):101.

[34] Chang CJ, Chao CH, Xia W, et al. p53 regulates epithelial-mesenchymal transition and stem cell properties through modulating miRNAs. Nat Cell Biol. 2011 Mar;13(3):317-23.

[35] Chang CJ, Chao CH, Xia W, et al. p53 regulates epithelial-mesenchymal transition and stem cell properties through modulating miRNAs. Nat Cell Biol. 2011 Mar;13(3):317-23.

[36] Lee KM, Nam K, Oh S, et al. ECM1 regulates tumor metastasis and CSC-like property through stabilization of β-catenin. Oncogene. 2015 Dec 10;34(50):6055-65.

[37] Wu Q, Chen D, Luo Q, Yang Q, Zhao C, Zhang D, Zeng Y, Huang L, Zhang Z, Qi Z. Extracellular matrix protein 1 recruits moesin to facilitate invadopodia formation and breast cancer metastasis. Cancer Lett. 2018 Nov 28;437:44-55.

[38] Park J, Kim DH, Shah SR, Kim HN, Kshitiz, Kim P, Quiñones-Hinojosa A, Levchenko A. Switch-like enhancement of epithelial-mesenchymal transition by YAP through feedback regulation of WT1 and Rho-family GTPases. Nat Commun. 2019 Jun 26;10(1):2797.

Tables

Table1 Relationship between ROBO2 expression and clinicopathological characteristics in pancreatic cancer patients.

Variables	Number（n）	ROBO2 expression		*P* value
		High group	Low group	
Gender				0.416
Male	49	20	29	
Female	46	18	28	
Age,y				0.596
≥60	40	17	23	
<60	55	21	34	
CA19-9 level				0.720
Normal	66	25	41	
Elevated	29	13	16	
Tumor size				0.641
≤4	52	21	31	
>4	43	17	28	
Tumor location				0.492
Head	62	26	36	
Body-tail	33	12	21	
Differential degree				0.945
High/moderate	58	22	36	
Low	44	16	28	
Perineural invasion				0.630
Absent	27	11	16	
Present	63	26	36	
Vessel invasion				0.065
Absent	59	24	25	
Present	32	13	19	
T stage				0.273
T1-2	31	12	19	
T3	64	26	38	

N stage				0.089
N0	51	20	31	
N1	44	18	26	

P value in bold is statistically significant. The total patient number dose not equal to 95 for all variables due to a lack of patient information in some cases. T, tumor; N, lymph node; ROBO2, roundabout receptor 2.

Table 2 Univariate and multivariate analyses for prognosis factors in PDAC

Variables	Numbers(n)	HR	Univariate analysis		Multivariate analysis		
			95%CI	*P* value	HR	95%CI	*P* value
Gender							
Male	49	1					
Female	46	1.132	0.580-2.211	0.256			
Age,y							
≥60	40	1					
<60	55	0.988	0.962-1.015	0..389			
CA19-9 level							
Normal	66	1					
Elevated	29	0.995	0.988-1.001	0.110			
Tumor size							
≤4	52	1					
>4	43	0.864	0.703-1.062	0.166			
Tumor location							
Head	62	1					
Body-tail	33	1.253	0.747-2.101	0.457			
Differential degree							
High/moderate	58	1					
Low	44	0.976	0.650-1.473	0.905			
Perineural invasion							
Absent	27	1					
Present	63	0.968	0.466-2.009	0.603			
Vessel invasion							

Absent	59	1					
Present	32	1.801	0.946-3.426	0.498			
T stage							
T1-2	31	1					
T3	64	0.935	0.456-1.916	0.983			
N stage							
N0	51	1			1		
N1	44	2.271	1.245-4.142	**0.007**	3.351	1.781-6.305	**<0.001**
ROBO2 expression							
Low	38	1			1		
High	67	0.463	0.292-0.615	**<0.001**	0.392	0.249-0.652	**<0.001**

The total patient number does not equal 95 for all variables, as patient information was not available in some cases.

HR, hazard ration; T, tumor; N, lymph node; PDAC, pancreatic ductal adenocarcinoma;

Figures

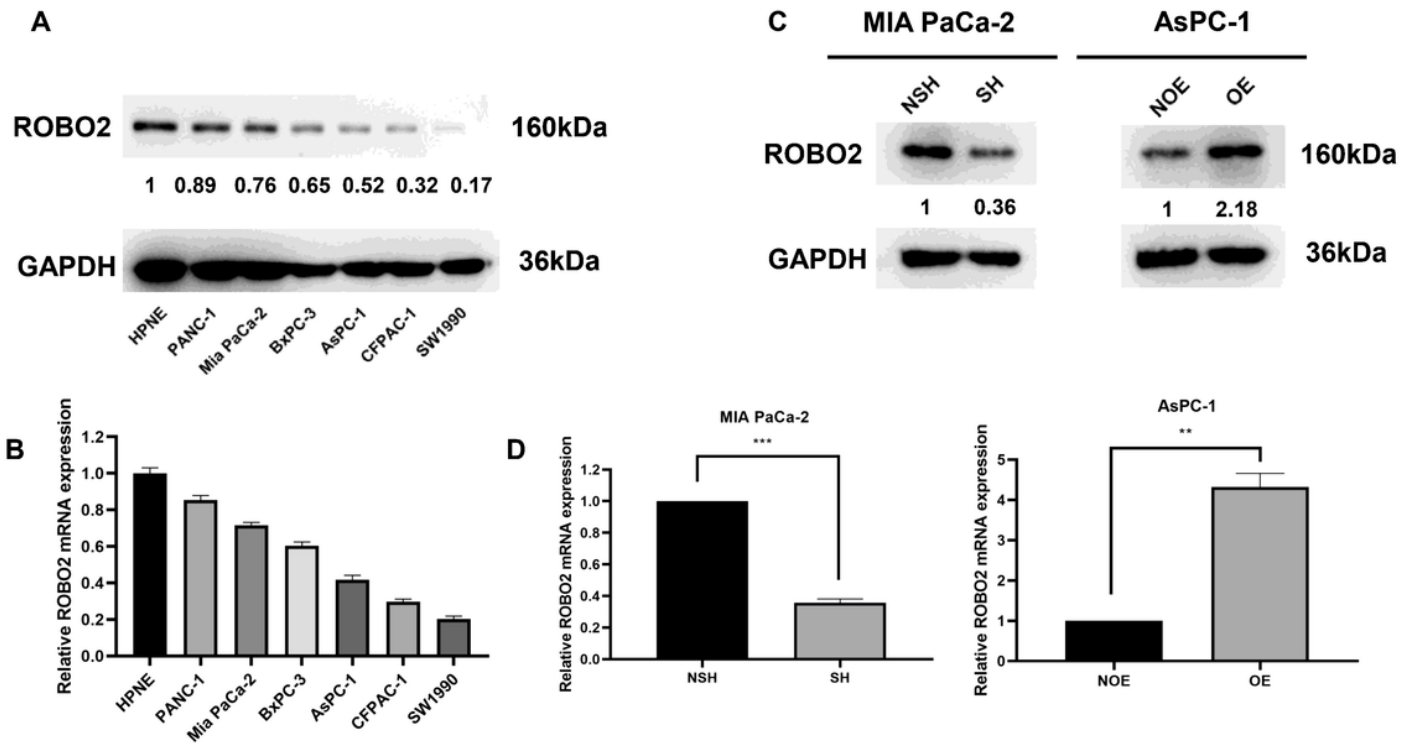

Figure 1

Selection of MIA PaCa-2 and AsPC-1 cell lines establishment of cell lines by transient transfection for ROBO2 knockdown or expression. (A) ROBO2 protein expression in HPNE and six PDAC cell lines. (B) ROBO2 mRNA expression level in HPNE and six PDAC cell lines. (C, D) The efficacies of ROBO2 knockdown and expression confirmed by western blot and RT-PCR analyses. Data are presented as mean ± SD. **P < 0.01, ***P < 0.001, by Student's t-test. PDAC, pancreatic ductal adenocarcinoma; SH, ROBO2 knockdown; NSH, scrambled control; OE, ROBO2 overexpression; NOE, negative control for ROBO2 overexpression (n=3).

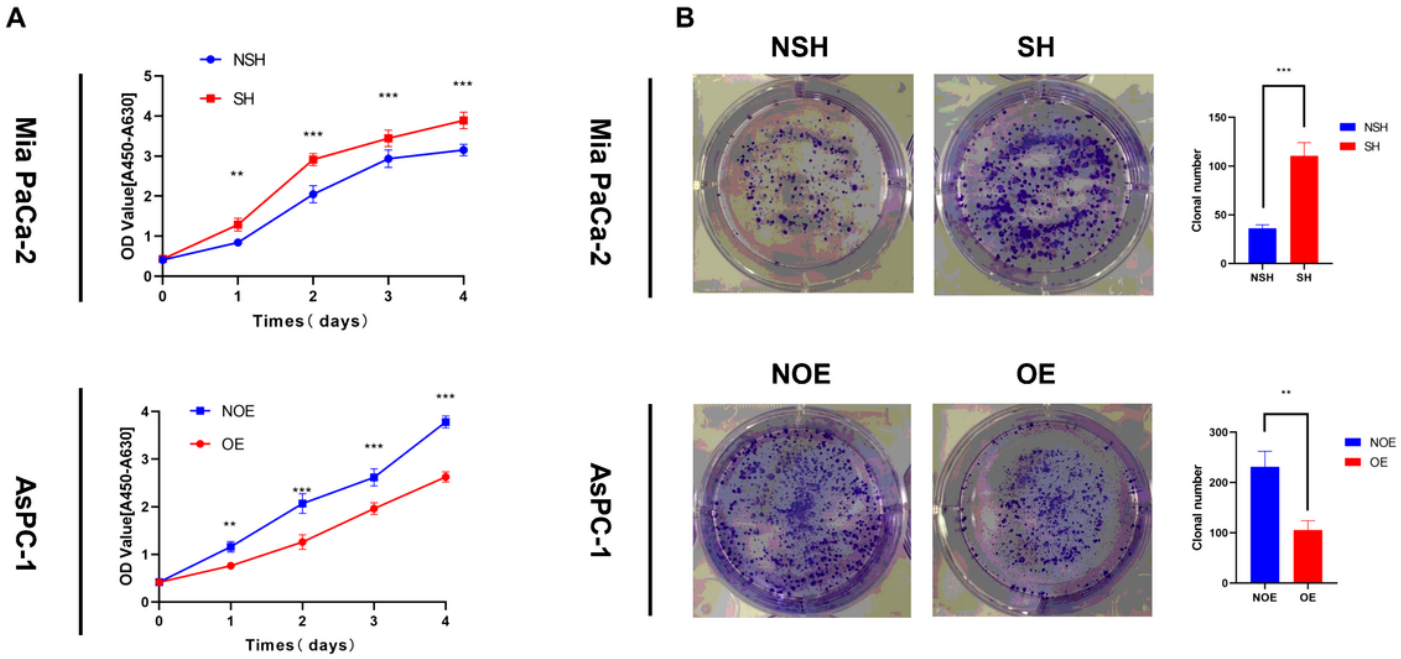

Figure 2

ROBO2 inhibits PDAC cell proliferation in vitro. (A) Cell proliferation evaluated by CCK-8 assays in MIA PaCa-2 and AsPC-1 cell lines. (B) Clonal formation assays detected the MIA PaCa-2 and AsPC-1 cells proliferation. Data are presented as mean ± SD. **P < 0.01, ***P < 0.001, by Student's t-test. CCK-8, Cell Counting Kit-8; PDAC, pancreatic ductal adenocarcinoma; SH, ROBO2 knockdown; NSH, scrambled control; OE, ROBO2 overexpression; NOE, negative control for ROBO2 overexpression (n=3).

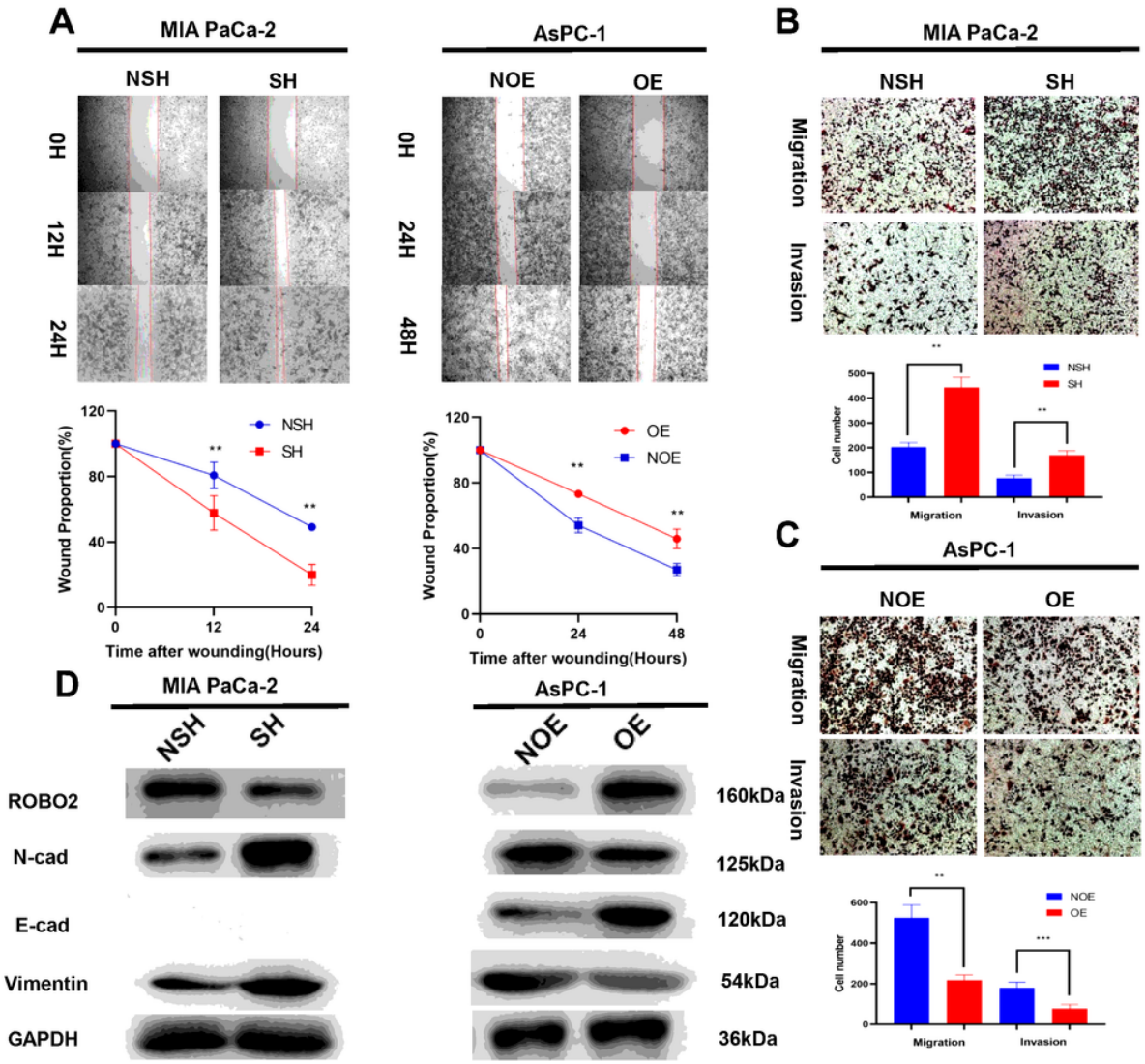

Figure 3

ROBO2 hampers PDAC cell migration and invasion in vitro. (A) Cell migration abilities of MIA PaCa-2 and AsPC-1 cell were investigated by wound healing assays. (B, C) In vitro transwell migration and invasion assays were performed in MIA PaCa-2 and AsPC-1 cell lines. Representative images are shown. Magnification, 100×. Cell numbers of migrated and invasive cell are shown in the bottom panels. (D) ROBO2 overexpression promoted E-cadherin expression and decreased vimentin and N-cadherin, while ROBO2 knockdown had the opposite effects. MIA PaCa-2 cell did not express E-cadherin.

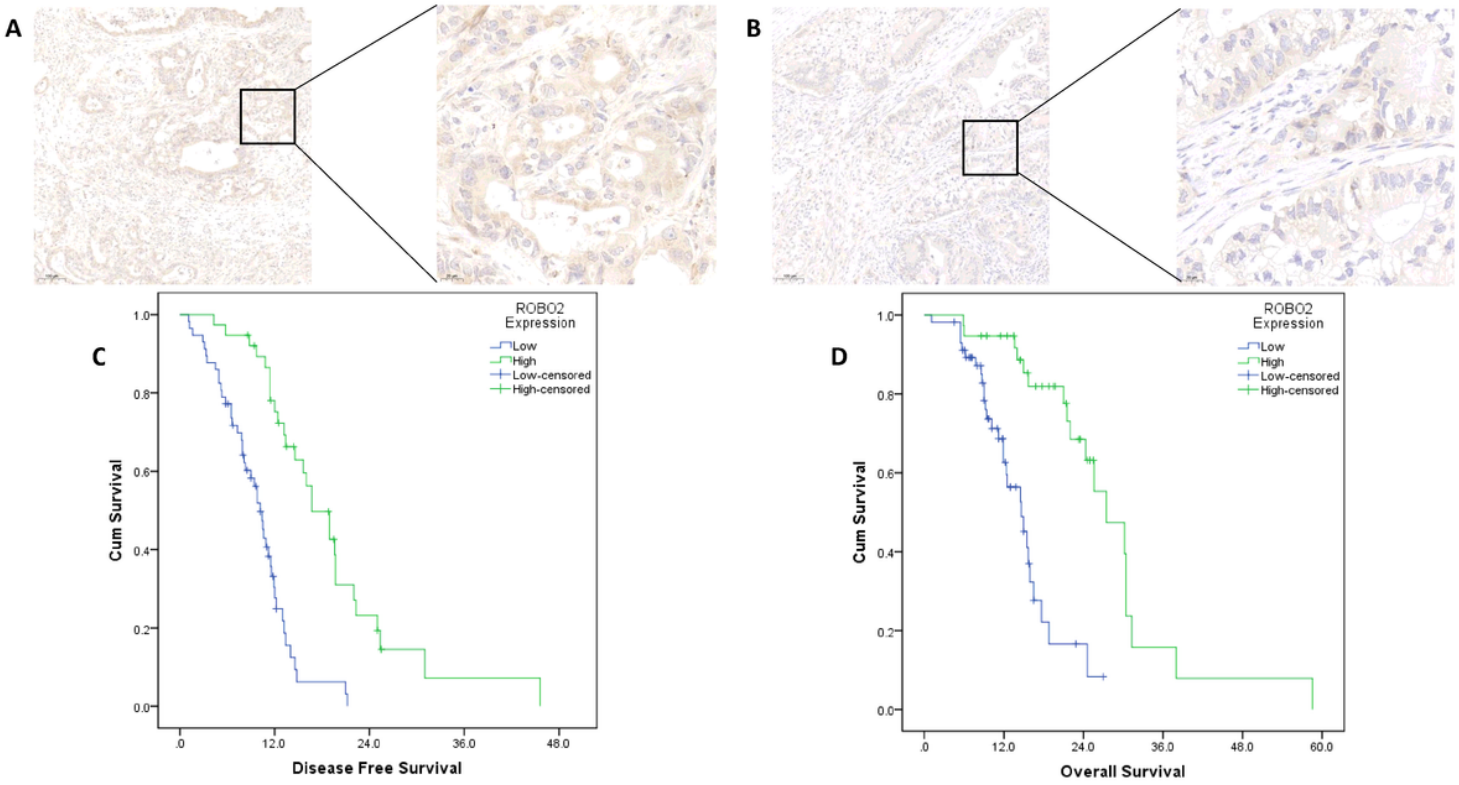

Figure 4

IHC results of ROBO2 expression in PDAC tissues and Kaplan-Meier curve of disease-free survival and overall survival according to the expression level of ROBO2. (A, B) The expression level of ROBO2 in two PDAC samples. (C, D) Kaplan-Meier survival curve of the effect of ROBO2 level on disease-free survival (P = 0.002; log-rank test) and overall survival (P< 0.001; log-rank test).

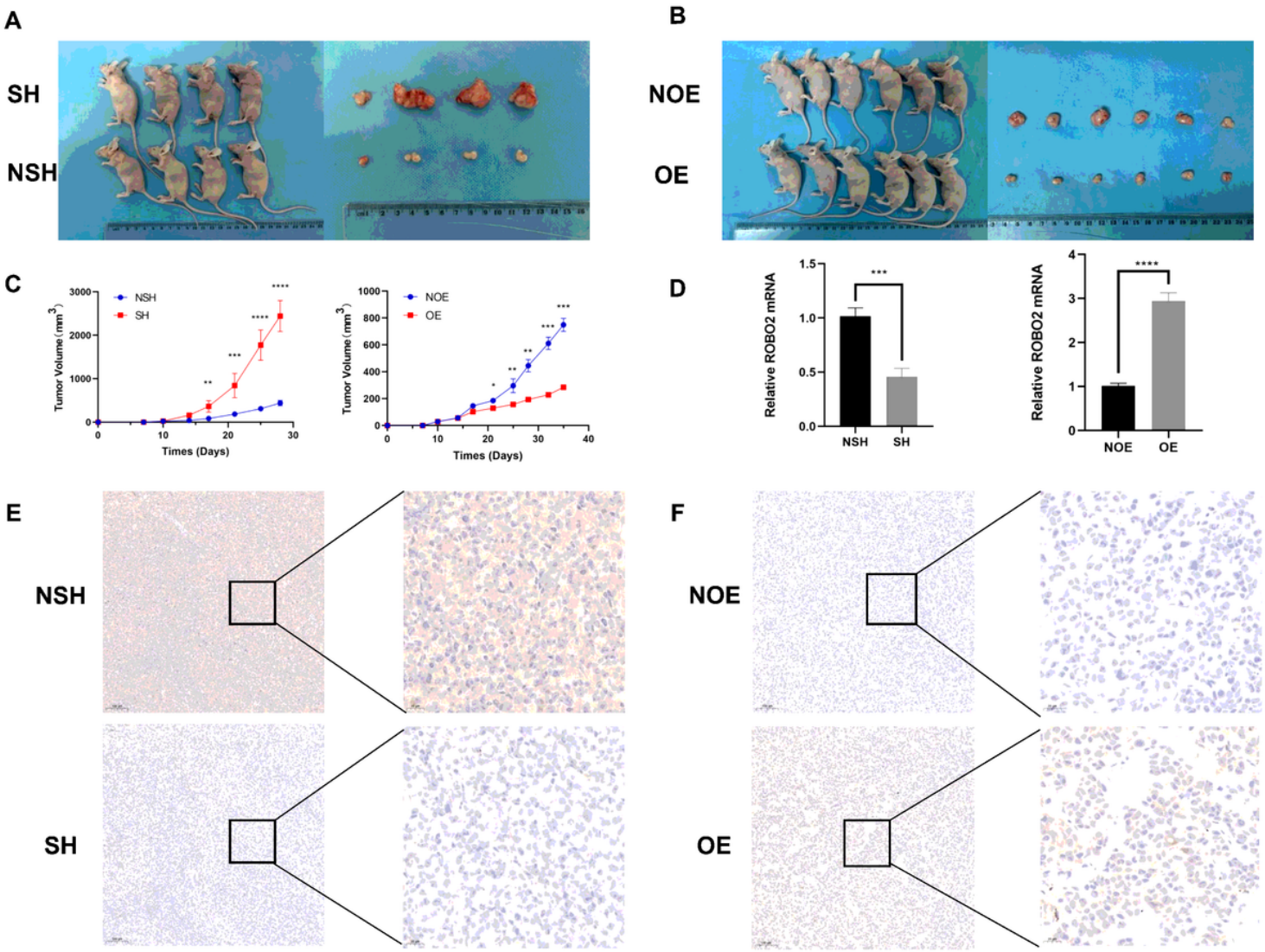

Figure 5

ROBO2 inhibits PDAC cell proliferation in vivo. (A, B) ROBO2 knockdown promotes tumor growth while ROBO2 overexpression inhibits tumor growth in vivo. (C) The tumor volume of ROBO2 knockdown and overexpression were shown in the panel. (D) RT-PCR was used to confirm the expression of ROBO2 mice tumors. (E, F) IHC stating of ROBO2 in xenograft tumor tissues. Scale bar, 100μm. Data are presented as mean ± SD. *P < 0.05, **P < 0.01, ***P < 0.001, ****P < 0.001, by Student's t-test.

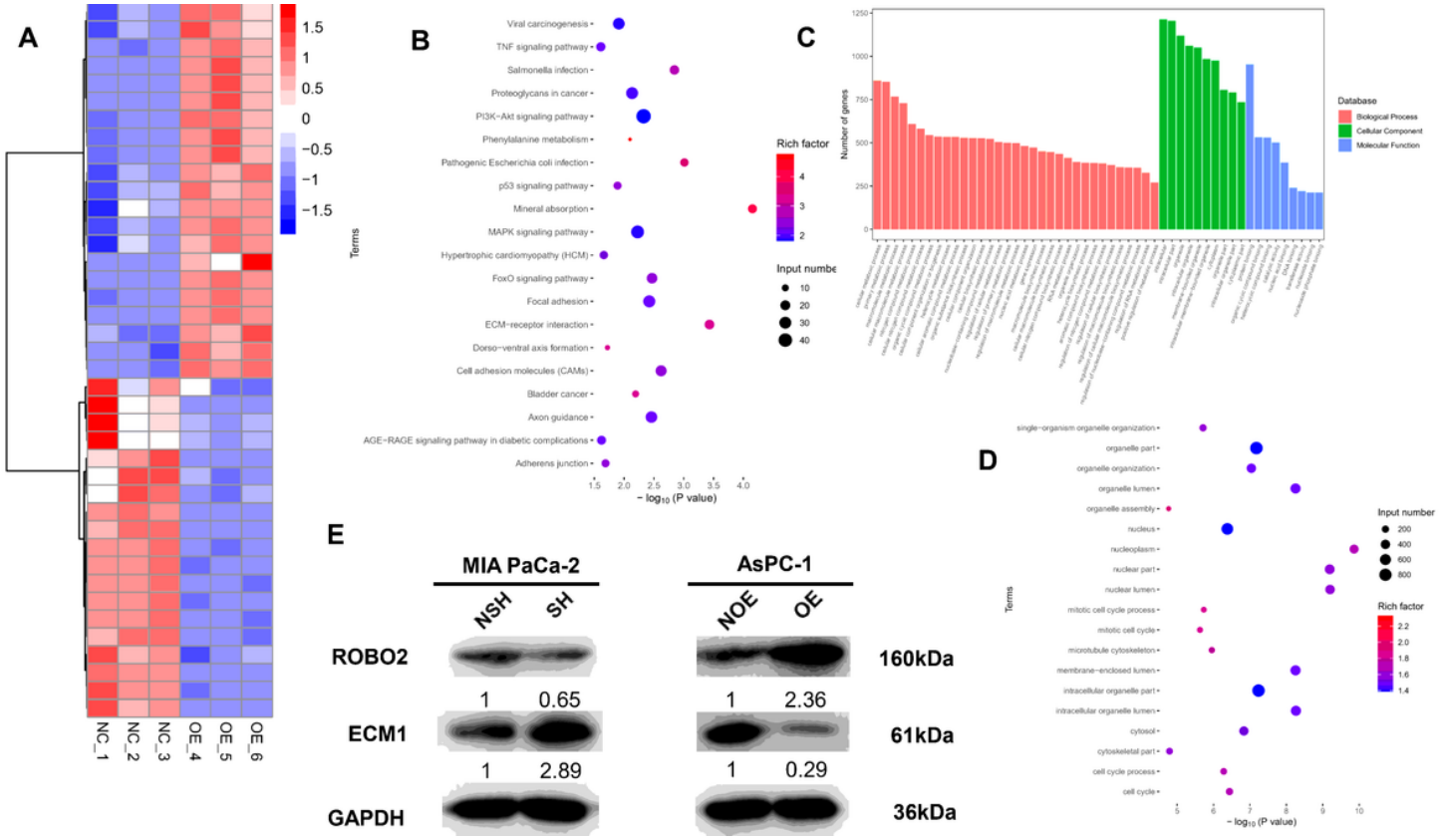

Figure 6

Bioinformatic screening and western blot revealed the potential targeted molecules of ROBO2 in PDAC. (A) Gene transcription profiles of genes regulated by ROBO2 in AsPC-1 cells. (B) KEGG pathway enrichment of differentially expressed genes. (C, D) GO enrichment analyses of differentially expressed genes regulated by ROBO2. (E) Western blot investigate the protein expression of ECM1 in MIA PaCa-2 and AsPC-1 cell lines. ECM1, extracellular matrix protein-1.